Proteasome and VCP inhibition blocks necroptosis in HT-29 cells

A thesis submitted by

Kerem Cahit Gürol

in partial fulfillment of the requirements for the degree of

Master of Science

in

Pharmacology and Drug Development

Tufts University

Sackler School of Graduate Biomedical Sciences

May 2018

Advisor: Alexei Degterev, PhD

Abstract

Necroptosis is a programmed form of cell death mediated by the formation of a detergent-insoluble protein complex called necrosome. Receptor Interacting Protein Kinases (RIPK) 1 and 3 have been identified as the key components of the necrosome. Phosphorylation and ubiquitination of several RIPK1/3 residues have been implicated to play important roles in regulating apoptosis and necroptosis.

As the main mechanism for cellular protein degradation, ubiquitin-proteasome system (UPS) has been associated with a myriad of cellular pathways, including apoptosis. However, the mechanism and function of UPS under apoptotic or necroptotic conditions are poorly understood.

In the present study we report that proteasome inhibitor bortezomib and Valosin-Containing Protein (VCP) inhibitor NMS-873 inhibit necroptosis in human colorectal cancer HT-29 cells. We claim that this action is due to VCP inhibition altering the ubiquitination profile of RIPK1 and RIPK3 in the necrosome. RIPK1 interacts with VCP upon TNFα stimulation in a complex separate from the necrosome or TNF Receptor 1 signaling complex.

Table of Contents

List of Figures

List of Abbreviations

FADD: Fas-associated Protein with Death Domain
IAP: Inhibitor of Apoptosis Protein
IKK: IκB Kinase
KO: Knock-out
LUBAC: Linear Ubiquitin Assembly Complex
MAPKAPK2 (MK2): MAP Kinase-activated Protein Kinase 2
MLKL:Mixed Lineage Kinase-Like
NFκB: Nuclear Factor Kappa B
PAMP: Pathogen-associated Molecular Pattern
RHIM: RIP Homotypic Interaction Motif
RIPK1: Receptor Interacting Protein Kinase 1
RIPK3: Receptor Interacting Protein Kinase 3
SM:Smac Mimetic
TNF: Tumor Necrosis Factor
TNFR1: Tumor Necrosis Factor Receptor 1
TIS: TNFα, IDN-6556, Smac mimetic-164
TRADD:Tumor Necrosis Factor Receptor 1-associated Death Domain
TRAF2: Tumor Necrosis Factor Receptor-associated Factor 2
UPS: Ubiquitin-Proteasome System
VCP:Valosin-Containing Protein

Chapter 1: Introduction

1.1 Mechanism and Regulation of TNFα-induced Necroptosis

Necroptosis is a programmed form of necrotic cell death mediated by an insoluble, amyloid-like protein complex called necrosome. The activity of serine/threonine kinases Receptor Interacting Protein Kinase 1 (RIPK1) and Receptor Interacting Protein Kinase 3 (RIPK3) are required for the formation of the necrosome, which leads to the phosphorylation and activation of the downstream effector protein called Mixed Lineage Kinase Domain Like (MLKL) (Sun et al. 2012). Phosphorylated MLKL oligomerizes and translocates to the plasma membrane, initiating cell death by compromising the integrity of the membrane (Hildebrand et al. 2014).

While necroptosis can be triggered by multiple PAMPs and cytokines, the mechanism of Tumor Necrosis Factor α (TNFα) induced necroptosis signaling pathway has been most extensively studied and understood. Binding of TNFα to TNF Receptor 1 (TNFR1) recruits a membrane bound complex called Complex I, which consists of RIPK1 as well as TNFR1-associated Death Domain (TRADD) and TNF Receptor-associated Factor 2 (TRAF2). E3 ubiquitin ligases such as Linear Ubiquitin Chain Assembly Complex (LUBAC) and Inhibitor of Apoptosis Proteins (IAP) cIAP1 and cIAP2 are recruited to the complex to ubiquinate RIPK1. Polyubiquitinated RIPK1 is recognized by NF-κB activating factors TAK1 and IκB Kinase (IKK) family proteins, leading to transcription of inflammatory, pro-survival genes (DiDonato et al. 1997).

Deubiquitination of RIPK1 or inhibition of cIAPs by smac mimetics (SM) promotes formation of the cytosolic, pro-death complex called Complex II, which consists of RIPK1, Procaspase-8, and Fas-associated Protein with Death Domain (FADD)

(Wang et al. 2008). SMs are potent and highly selective small molecule inhibitors of IAPs that mimic the activity of SMAC protein, a natural inhibitor of IAPs. Depending on several factors, Complex II may lead to RIPK1 kinase dependent/independent apoptosis, or form the necrosome (Complex IIb), inducing necroptosis. Protein synthesis inhibition by cycloheximide promotes RIPK1-independent apoptosis initiated by Caspase-8 processing. Inhibition of Caspase-8, however, promotes necroptosis, which requires the kinase activity of both RIPK1 and RIPK3 (He et al. 2009). In addition to playing a role in NFκB activation, TAK1 has been also associated with favoring necrosome formation by mediating phosphorylation of RIPK1 at Ser321. In the absence of TAK1-mediated Ser321 phosphorylation, RIPK1-dependent apoptosis is favored by preferential RIPK1 association with Caspase adaptor protein FADD (Geng et al. 2017). Lastly, inhibition of IAPs in Complex I has been shown to promote pro-apoptotic activity of Complex II, which is mediated by the kinase function of RIPK1.

While the exact structure of the necrosome, or the mechanism of its formation are yet to be elucidated, RIPK1-RIPK3 interaction has been proven to be crucial for necrosome formation and function. RIPK1 binds RIPK3 through a highly homologous RIP homotypic interacting motif (RHIM) domain (Sun et al. 2002). In addition, phosphorylation and kinase activity of both RIPK1 and RIPK3 are essential for necroptosis, as treatment with RIPK1 kinase inhibitor Necrostatin-1 (Nec-1) or RIPK3 kinase inhibitor GSK'872 is sufficient to inhibit necroptosis (Degterev et al. 2005; Mandal et al. 2014). Phosphorylation of RIPK1 and RIPK3 has been suggested to expose buried RHIM domains, resulting in the formation of an amyloid-like RIPK1-RIPK3 necrosome core. In return, more RIPK1 and RIPK3 are incorporated into the necrosome

core by auto- and cross phosphorylation of RIPK1/3 (Li et al. 2012).

As summarized above, post-translational modifications - especially phosphorylation and ubiquitination - of RIPK1 and RIPK3 have important regulatory roles in the response to TNFα signaling. Whereas RIPK1 ubiquitination in Complex I promotes cell survival by NFκB signaling, polyubiquitination of several sites on RIPK1 and RIPK3 in the necrosome have also been reported. However, the inhibitory or stimulatory functions of these modifications are not clearly defined yet (Moquin et al. 2013; Ozinawa et al. 2015). Interestingly, phosphorylation and ubiquitination of RIPK1 in the necrosome are also reported to regulate each other. RIPK1 KO HT29 cells expressing RIPK1 with a mutated ubiquitination site on Lys115 showed NFκB activation and RIPK1 ubiquitination in Complex I comparable to wild-type cells. However, Lys115 mutation attenuated RIPK1 phosphorylation in Complex II, protecting the cells against necroptosis (de Almagro et al. 2017).

1.2 Role of Ubiquitin-Proteasome System in Apoptosis Regulation

The role of Ubiquitin-Proteasome System (UPS) in apoptosis has been studied extensively over the last two decades. Specifically, the E3 ubiquitin ligase activity of IAPs has been studied because of their role in inhibiting apoptosis; either by inhibition or proteasomal degradation of caspases (Bader, M., and Steller, H. 2009). Conversely, auto-ubiquitination derived degradation of IAPs induced by IAP antagonists such as SMs has been shown to promote apoptosis (Varfolomeev et al. 2007). Due to upregulated IAP levels associated with several cancer types, SMs have also garnered attention as potential antitumor therapeutics with multiple ongoing clinical trials (Fulda, S., and Vucic, D. 2012).

In addition to IAP antagonists, proteasome inhibitors have also emerged as potential cancer drugs. 26S proteasome inhibitor Bortezomib was approved as the first therapeutic proteasome inhibitor for multiple myeloma (Chen et al. 2011). Bortezomib-induced apoptosis has been attributed to suppression of NFκB signaling by preventing proteasomal degradation of NFκB inhibitory IκB proteins (Adams, J., and Kauffman, M. 2004). However, recent studies suggest that NFκB inhibition does not play a critical role in the mechanism of bortezomib-induced apoptosis, as bortezomib is shown to activate NFκB instead of suppressing it *in vitro* in multiple myeloma cells (Hideshima et al. 2009).

Valosin-Containing Protein (VCP) is another key element of the UPS that has been reported to be involved in apoptosis regulation. Besides its diverse functions in cell cycle regulation and membrane fusion, VCP has been primarily associated with protein degradation by chaperoning ubiquitinated protein complexes to the proteasome (Wang et al. 2006). Initial experiments with loss-of-function mutations of CDC48, the yeast orthologue of VCP, showed pro-apoptotic markers, whereas elevated VCP levels have been associated with apoptosis resistance of several cancer tissues (Braun, R.J., and Zischka, H. 2008). Upregulated VCP expression in osteocarcoma cell lines has been suggested to protect against TNFα induced cell death by constant hyperactivation of NFκB signaling (Asai et al. 2002). More recently, NMS-873 was identified as a potent, allosteric inhibitor of VCP that induces apoptosis by endoplasmic reticulum (ER) stress in HCT116 colorectal carcinoma cells (Magnaghi et al. 2013).

1.3 Bridging the Gap between Necroptosis and Ubiquitin-Proteasome System

With a better understanding of the regulatory roles of RIPK1/3 phosphorylation and ubiquitination in determining cell death over the last few years, the ubiquitin-proteasome system also emerged as a potential therapeutic target for necroptosis promotion or suppression. Smac mimetic BV6 has been shown to synergize with bortezomib to trigger cell death in B-cell non-Hodgkin lymphoma cells in the presence or absence of caspase-8 inhibition (Bhatti et al. 2017). Bortezomib and MG132, another proteasome inhibitor, activated the necroptotic pathway even in the absence of caspase-8 inhibition in mouse fibroblasts (Moriwaki, K., and Chan, F.K. 2016).

In this study, we sought to understand the functional role of the ubiquitin-proteasome system on TNFα-induced necroptotic signaling using the proteasome inhibitor bortezomib and the VCP inhibitor NMS-873. In addition, we aimed to elucidate potential interactions of VCP with TNFα induced signaling complexes involving RIPK1/3.

Chapter 2: Materials and Methods

2.1. Cell Culture

Human colorectal adenocarcinoma cell line HT-29 and mouse macrophage cell line RAW 264.7 were cultured with 5% CO_2 at 37^0C in Dulbecco's Modified Eagle Medium, high glucose (DMEM) (Thermo Scientific, Cat. No. 11965) supplemented with 10% (v/v) Fetal Bovine Serum (FBS) (Sigma-Aldrich) and 1% 100x Antibiotic-Antimycotic (Thermo Scientific, Cat. No. 15240).

2.2 Reagents

IDN-6556 and SM-164 were dissolved in DMSO and used at final concentrations of 10µM and 1µM, respectively. NMS-873 was dissolved in DMSO and used at 3µM for HT-29 cells and 1µM for RAW 264.7 cells. Human and mouse TNFα were dissolved in PBS and used at 10ng/ml. TIS treated cells were harvested after 3 (RAW 264.7) or 4 (HT-29) hours for experiments involving Western blots.

2.3 Cell Viability Experiments

CellTiter-Glo® Luminescent Cell Viability Assay (Promega) was conducted according to the instructions provided by Promega.

2.4 Western Blotting

Cells were cultured in $10cm^2$ tissue culture plates to 75% confluency. Cultured cells were harvested in ice cold PBS and centrifuged at 4470g for 3 minutes. After removal of the supernatant, the pellet was lysed with Triton X-100 lysis buffer (0.05% Triton X-100, 150mM NaCl, 1mM EDTA, 20mM Tris-HCl pH 7.5, 3mM NaF, 1mM β-glycerolphosphate, 1mM Na_3VO_4, 1µg/ml aprotinin, 1µg/ml pepstatin, 1µg/ml leupeptin, 50µg/ml PMSF, and 5µM PR-619) by 15 minutes of incubation on ice with occasional,

brief vortexing. For experiments involving samples treated with TIS, all lysates were centrifuged at 1000g for 15 minutes at 4^0C. For all other experiments, lysates were centrifuged at 16,000g for 15 minutes at 4^0C. The protein concentrations of the collected supernatants were measured with Pierce 660nm Protein Assay Reagent (Thermo Scientific, Cat. No. 22660) and normalized with Triton X-100 lysis buffer to the lowest concentration or 2mg/ml. Normalized lysates were diluted with 4x SDS-PAGE loading buffer (200mM Tris-HCl pH 6.8, 8% (w/v) SDS, 40% (v/v) glycerol, 4% (v/v) β-mercaptoethanol, 50mM EDTA, 0.08% (w/v) bromophenol blue) and boiled on a heating block at 95^0C for 5 minutes.

After SDS-PAGE and transfer to PVDF membranes, the membranes were blocked with Pierce Protein-Free T20 Blocking Buffer (Thermo Scientific, Cat. No. 37571) at room temperature for 30 minutes and incubated with primary antibodies diluted in the same blocking buffer overnight at 4^0C. Membranes were washed three times for 10 minutes with TBST at room temperature. The secondary antibodies were also diluted in the same blocking buffer and incubated at room temperature for one hour. Membranes were washed three times for 20 minutes with TBST, incubated for 2 minutes in Luminata Forte (Millipore Sigma, Cat. No. WBLUF0500) or Luminata Classico (Millipore Sigma, Cat. No. WBLUC0500) Western HRP Substrates and visualized using the Konica SRX-101A film processor.

2.5 Detergent Insoluble Lysate Extract Preparation

After preparing a small portion of whole cell lysate samples for SDS-PAGE as described in the Western Blotting section, the remaining cell lysate was centrifuged at 16,000g for 15 minutes at 4^0C. The supernatant containing detergent soluble lysate

extract was diluted in 4x SDS-PAGE loading buffer and heated at 95^0C for 5 minutes. The isolated pellet was resuspended in Triton X-100 lysis buffer and centrifuged again with the same settings. The pellet was resuspended in 1x SDS-PAGE loading buffer and heated at 95^0C for 5 minutes.

2.6 Immunoprecipitation

For RIPK1 immunoprecipitation, both rabbit (1:100) RIPK1 (Cell Signaling, Cat. No. 3493) and mouse (1:200) RIPK1 (Abcam, Cat. No. ab72139) antibodies were added to the normalized cell lysates and incubated overnight at 4^0C. Pierce Protein A Magnetic Beads (Thermo Scientific, Cat. No. 88845) were washed twice with Triton X-100 lysis buffer and incubated with the lysate-antibody samples at 4^0C for two hours. After collecting the supernatant containing the unbound lysate fragment, the beads were washed twice with Triton X-100 lysis buffer supplemented with 500mM NaCl and eluted with 1x SDS-PAGE loading buffer.

Complex I immunoprecipitation using FLAG-tagged human TNFα (Adipogen, Cat. No. 40B-0006) was conducted as described before (Dziedzic et al. 2017).

For pulldown of 3x FLAG-hVCP HA-Ub HT29 cells, the whole cell lysates were normalized as described above. Pierce Anti-DYKDDDDK Magnetic Agarose beads (Thermo Scientific, Cat. No. A36797) were washed twice with Triton X-100 lysis buffer and incubated with the lysates for 3 hours at 4^0C. After collecting the supernatant containing the unbound lysate fragment, the beads were washed three times with Triton X-100 lysis buffer and eluted by incubation with 250µg/ml 3x FLAG Peptide (ApexBio, Cat. No. A6001) diluted in Triton X-100 lysis buffer at 4^0C for 1 hour.

2.7 Statistical Analysis

The statistical significance of the viability experiments was analyzed by two-tailed paired Student's t-test.

Chapter 3: Results

3.1 NMS-873 protects HT-29 cells against TNFα induced necroptosis

We sought to determine the functional effects of allosteric VCP inhibitor NMS-873 on human colorectal adenocarcinoma (HT-29) and mouse macrophage (RAW 264.7) cell line viability under TNFα induced necroptotic conditions. After 6 hours, NMS-873 on its own did not cause significant toxicity to either cell type (Figure 3.1a). In the absence of NMS-873, treatment with either mouse or human TNFα (T) supplemented with pan-caspase inhibitor IDN6556 (I) and smac mimetic SM164 (S) potently induced cell death for both cell lines. As expected, RIPK1 inhibition by Nec-1 (N), RIPK3 inhibition by GSK'872 (G), and combination of both inhibitors (NG) successfully inhibited TIS induced cell death. Interestingly, HT-29 cells were significantly protected against necroptosis with NMS-873 treatment, while RAW cells were slightly sensitized even in the absence of a smac mimetic.

As suspected, prolonged NMS-873 exposure severely reduced viability of both cell types after 24 hours (Figure 3.1b). Despite its toxicity, NMS-873 continued to, albeit poorly, protect HT-29 cells against necroptosis. While both cell types were potently protected against necroptosis by RIPK1 and RIPK3 inhibitor combination, the potency of each RIPK inhibitor on its own differed between cell lines. Nec-1 retained full protection of HT-29 cells, while GSK'872 completely protected RAW cells 24 hours after TIS treatment. Interestingly, NMS-873 treatment in combination with GSK'872 significantly reduced cell death in HT-29 cells that were only partially protected by GSK'872.

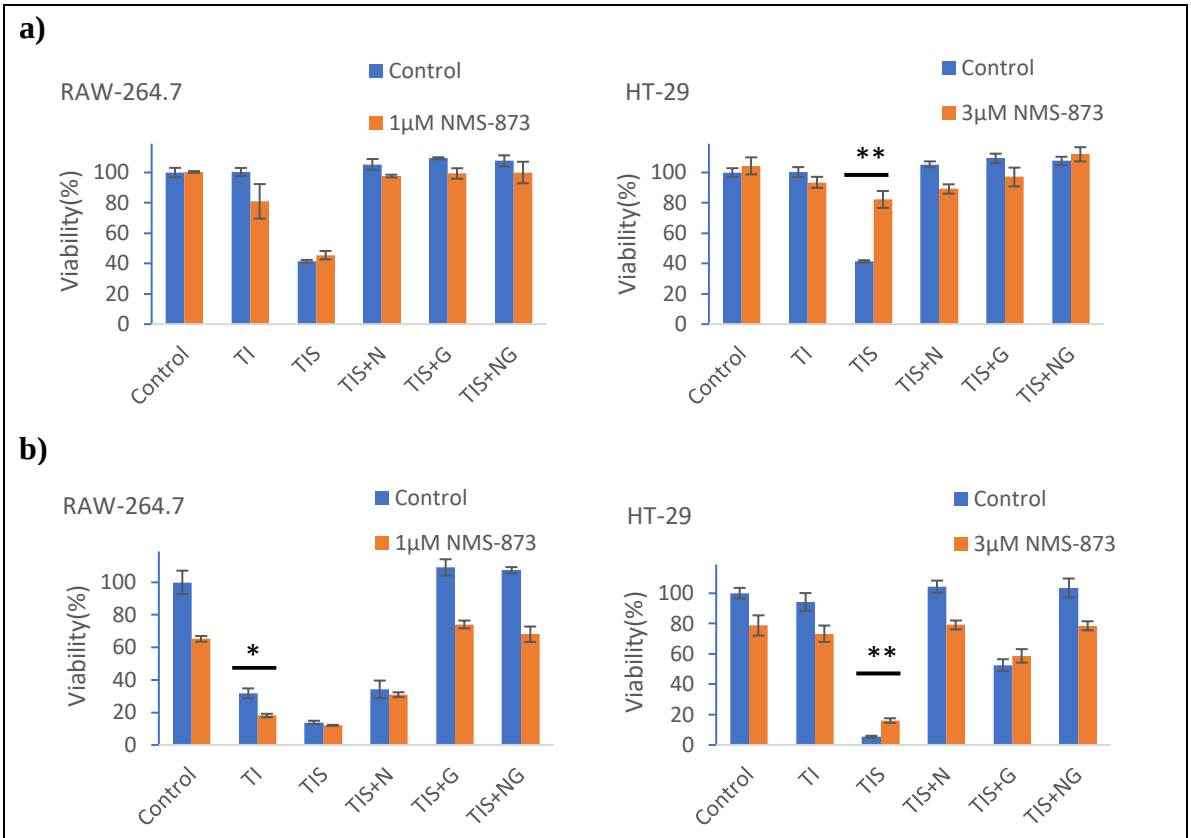

Figure 3.1 VCP inhibitor protects HT-29 cells after a) 6 hours and b) 24 hours of TIS treatment. The experiment was conducted in triplicates. Each point of triplicates was normalized to the mean luminescence signal of DMSO treated control (leftmost blue) cells and presented as mean of normalized triplicates ± SD (*P<0.05; **P<0.005).

3.2 HT-29 and RAW cell necrosomes show different RIPK1/3 modification profiles upon VCP inhibition

To investigate the mechanistic effects of VCP inhibition in necroptosis, we isolated the detergent-insoluble lysate extracts from HT-29 and RAW cells treated with TIS in the presence or absence of VCP, Nec-1, and GSK'872. As expected, RIPK1 appears enriched with a ladder of bands indicative of poly-ubiquitination in TIS treated cells. Consistent with the viability data, necroptosis effector protein MLKL is mainly activated in TIS treated cells in the absence of RIPK1/3 inhibition.

NMS-873 treatment enriches total and phosphorylated RIPK1, and RIPK3 in the insoluble fractions of RAW cells. However, the same proteins are diminished in HT-29 necrosome upon VCP inhibition (Figure 3.2). The reduced p-MLKL signal in HT-29 cells treated with NMS-873 confirms protection against necroptosis. As suggested by the viability data, RIPK3 inhibition by GSK'873 partially protects HT-29 cells against necroptosis.

Interestingly, the most drastic changes in the RIPK1 modification profiles of HT-29 cells were observed in combination of RIPK1 and VCP inhibition. On the other hand, RIPK3 inhibition in combination with NMS-873 significantly increased RIPK1 and RIPK3 signals in the necrosome compared to GSK'873 on its own in RAW cells. Altogether, these findings indicate distinctly different mechanisms of VCP regulation in necroptosis signaling for each cell line.

3.3 VCP interacts with RIPK1 prior to necrosome formation independent from Complex I

Based on the inhibitory effects of NMS-873, we sought to characterize any protein complex involving VCP-RIPK1 interaction in HT-29 cells under TNFα induced necroptotic signaling. Initial immunoprecipitation (IP) experiments pointed towards formation of a RIPK1-VCP complex after 15 minutes of TNFα treatment, where RIPK1 is presumed to be mainly incorporated into the membrane-bound Complex I. However, RIPK1-VCP interaction could not be consistently reproduced by following RIPK1 or VCP immunoprecipitation experiments, possibly due to the quick turnover of the complex. In addition, VCP was not detected as a part of Complex I with or without NMS-873 (Figure 3.3a-b).

In order to stabilize the VCP-RIPK1 complex, we sought to pre-treat TNFα-stimulated HT-29 cells with proteasome inhibitor bortezomib. VCP was strikingly enriched in RIPK1 IP eluate of TNFα-stimulated HT-29 cells pre-treated with bortezomib (Figure 3.3c). In addition, bortezomib significantly attenuated RIPK1 modification in necroptotic (TIS) HT-29 cells similar to NMS-873.

3.4 Bortezomib blocks necroptosis in HT-29 cells; activates MK2

Based on the decrease of modified RIPK1 signal observed in bortezomib pre-treated cells, we aimed to determine whether bortezomib protects HT-29 cells from necroptosis. Indeed, bortezomib pre-treatment significantly protected TIS treated cells against necroptosis (Figure 3.4). However, bortezomib-induced apoptosis significantly reduced HT-29 viability. Interestingly, less cell death was observed with 21 hours of TIS treatment and bortezomib pre-treatment than bortezomib pre-treatment alone due to protection against apoptosis by IDN-6556.

MAPKAPK2 (MK2) is a serine/threonine kinase that is involved in inflammatory response and NFκB activation (Gorska et al. 2007). A recent study showed MK2 dependent phosphorylation of cytosolic RIPK1 to inhibit the pro-death activity of RIPK1, thereby limiting Complex II and necrosome formation (Jaco et al. 2017). Since our findings also pointed towards the existence of a RIPK1-VCP complex that regulates RIPK1 associated cell death independent from Complex I, we aimed to determine whether proteasome or VCP inhibition activates MK2. Our initial findings show that MK2, and its upstream kinase p38, are activated in the presence of bortezomib and NMS-873 (Figure 3.5). However, it is yet unclear whether TNFα stimulation along with either

inhibitor affects MK2 activation. In addition, MK2 has not been detected in complex with RIPK1 or VCP by immunoprecipitation so far.

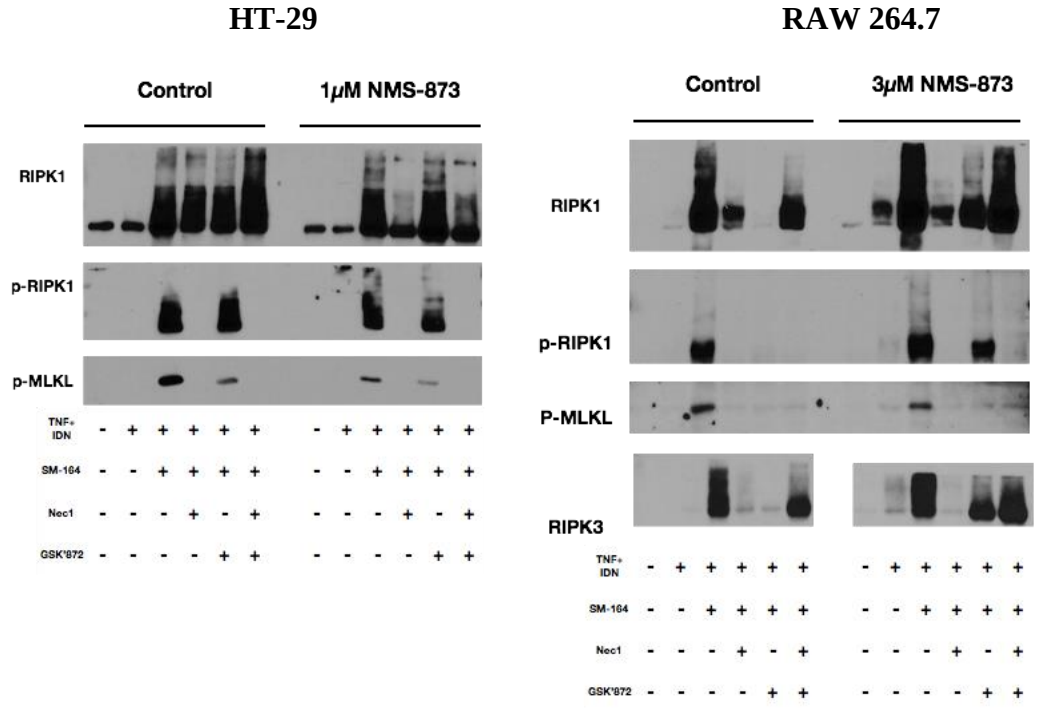

Figure 3.2 VCP inhibition drastically changes RIPK modification profile of the necrosome in both HT-29 and RAW cells. Western blot analysis of HT-29 and RAW 264.7 insoluble lysate fractions after 3 (RAW) or 4 (HT-29) hours of treatment with the specified compounds.

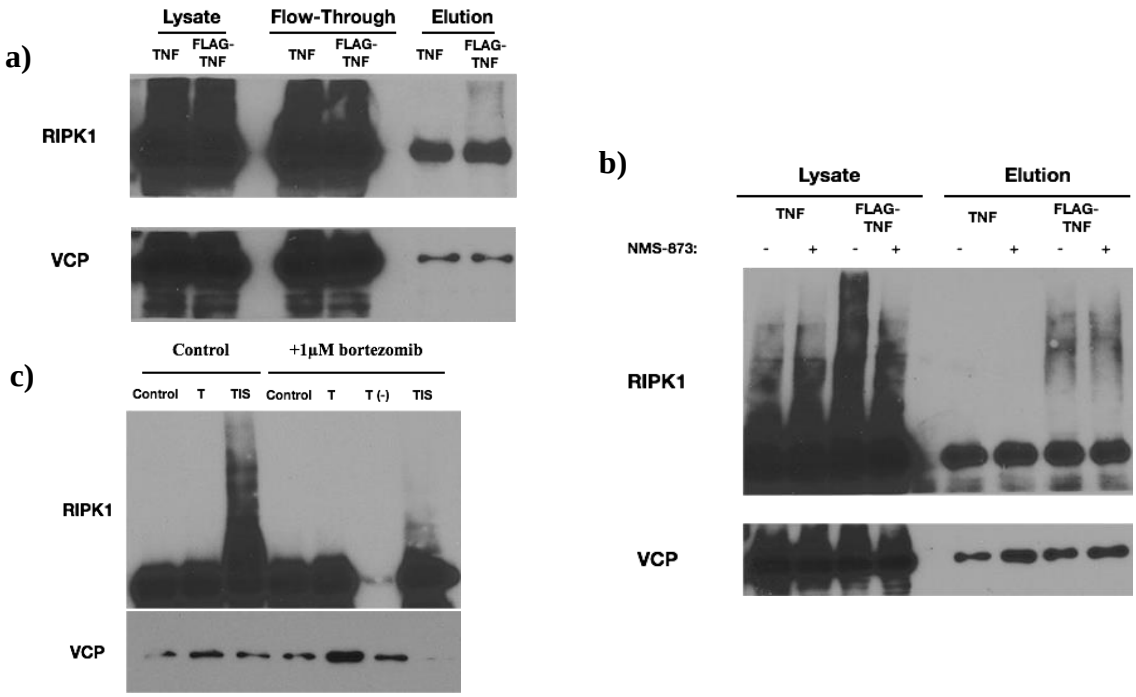

Figure 3.3 VCP binds to RIPK1 in a complex separate from Complex I or necrosome in the presence of bortezomib

a) Western blot analysis of TNF-induced Complex I immunoprecipitation. Cells were treated with 100ng/ml hTNF or FLAG-hTNF for 15 minutes prior to FLAG immunoprecipitation. VCP is not enriched by FLAG-hTNF (Complex I) pulldown.

b) Western blot analysis of TNF-induced Complex I immunoprecipitation ±NMS-873. Cells were pre-treated with 3μM NMS-873 or DMSO for 30 minutes, followed by 15 minutes of 100ng/ml hTNF or FLAG-hTNF prior to FLAG immunoprecipitation. VCP is not enriched in Complex I with or without NMS-873.

c) Western blot analysis of RIPK1 immunoprecipitation eluates from HT-29 cells pre-treated for 15 minutes with bortezomib, followed by 15 minutes with hTNFα (T) or 4 hours with TIS. T (-) lysate was not incubated with RIPK1 antibody as a negative control.

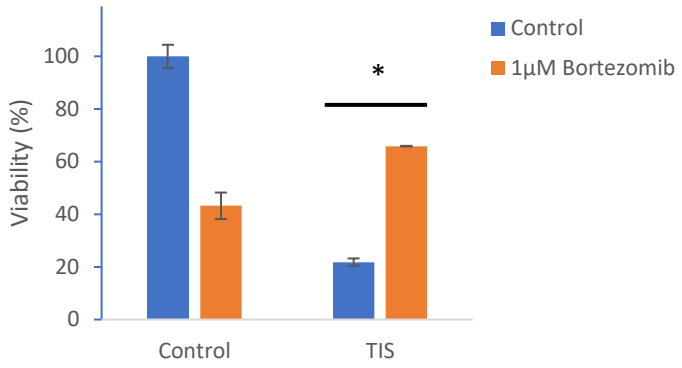

Figure 3.4 5-hour pre-treatment with 1µM bortezomib protects HT-29 cells from necroptosis. HT-29 cells were pre-treated with DMSO or bortezomib for 5 hours, followed by 21 hours of TIS treatment. Experiment was conducted in duplicates. Each data point was normalized to the mean of DMSO treated control cells. Each duplicate is presented as the mean of their normalized values in % Viability ±SD (*P<0.05).

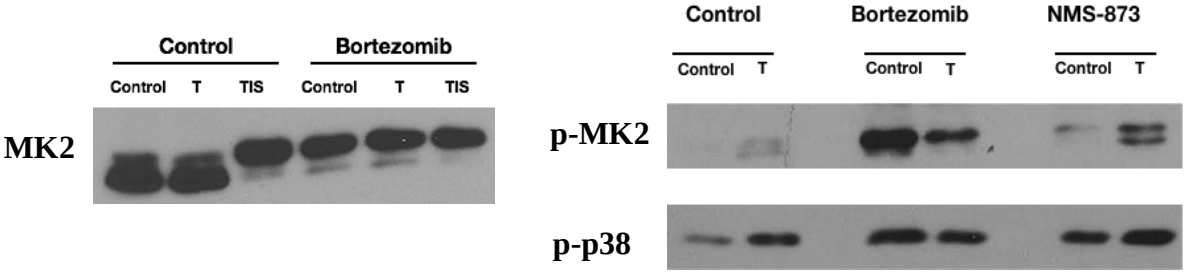

Figure 3.5 MK2 and p38 are activated constitutively by bortezomib and NMS-873 pre-treatment. Western blot analysis of HT-29 lysates pre-treated with bortezomib or NMS-873, followed by 15 minutes of hTNFα treatment (T) or 4 hours of TIS treatment.

Chapter 4: Discussion

Here we report that inhibition of VCP or 26S proteasome protects the human cancer cell line HT-29 from necroptosis. Overexpression of VCP has been suggested to play a pro-survival role in apoptotic conditions by promoting degradation of NFκB inhibitor IκB (Braun, R.J., and Zischka, H. 2008). We report that inhibition of VCP by NMS-873 results in reduced levels of polyubiquitinated RIPK1 and phosphorylated MLKL in the detergent-insoluble lysate fractions. Therefore, VCP likely plays a pro-necroptotic role in HT-29 cells upon TNF-stimulation combined with IAP and caspase-8 depletion.

VCP inhibition does not block necroptosis in mouse macrophage cell line RAW 264.7. Interestingly, NMS-873 increases RIPK1 and RIPK3 aggregates in the detergent-insoluble lysate fractions and slightly sensitizes RAW cells to necroptosis. Considering that both cell lines respond differently to RIPK1 and RIPK3 inhibition even in the absence of NMS-873, the RIPK1/3 composition of the necrosome might be highly variable among different cell types. Depending on whether RIPK1 or RIPK3 is more important for active necrosome formation in a specific cell line, VCP's involvement in ubiquitination or degradation of RIP kinases might either inhibit or promote necroptosis.

Since combination of RIPK1 and VCP inhibition drastically decreases RIPK1 ubiquitination profile compared to RIPK1 inhibition alone in HT-29 cells, VCP-RIPK1 interaction must be required for necrosome formation. Considering that we were only able to detect VCP-RIPK1 interactions after a short time span of TNF stimulation that is insufficient for RIPK3 containing death complexes to form, VCP might be preferentially interacting with RIPK1 during the transition from Complex I to II in HT-29 cells. Even

though VCP was not detected in Complex I, it might be transiently interacting with RIPK1 in Complex I and facilitating its transfer.

Further study of VCP-RIPK1 interaction in RAW cells is required to understand the dual function of VCP in necroptosis. Since VCP inhibition in combination with RIPK3 inhibitor GSK'872 drastically increases RIPK1, pRIPK1, and RIPK3 aggregation in RAW cells, VCP might preferentially bind to RIPK3 instead of RIPK1 in RAW cells. In that case, VCP likely plays a pro-survival role by promoting degradation of the growing necrosome aggregate.

As mentioned before, proteasome inhibitors have been studied for their pro-apoptotic effect in human cancer cell lines. Here we report that in addition to its pro-apoptotic role, proteasome inhibitor bortezomib blocks necroptosis in HT-29 cells. It is yet unclear whether bortezomib also attenuates cell death by inhibiting VCP-RIPK1 interactions. In addition, we have not yet characterized the effect of bortezomib on RIPK1/3 and pMLKL accumulation in the detergent-insoluble lysate fraction of either HT-29 or RAW cells.

Our initial findings suggest that proteasome or VCP inhibition results in activation of p38 and its downstream kinase, MK2 even in the absence of TNF signaling. This inhibitory effect is consistent with MK2's recently proposed role in suppressing RIPK1 recruitment to cytosolic death complexes (Jaco et al. 2017). As the next step in understanding the functional role of MK2 and p38 in necroptosis suppression, we expect inhibition of MK2 and p38 to restore necroptosis susceptibility to bortezomib treated HT-29 cells. In addition, TAK1, the upstream kinase of p38, might be also constitutively activated by proteasome inhibition. TAK1's pro-survival role in activating NFκB

signaling is well understood (Hayden, M.S., and Ghosh, S. 2008). More recently, TAK1 hyperactivation has been shown to drive RIPK3-dependent necroptosis. TAK1 Binding Protein 2 (TAB2) deficient fibroblasts show TAK1 hyperactivation and increased cell death after TNF stimulation, which is suppressed by RIPK3 inhibition (Morioka et al. 2014). TAB2 is a polyubiquitin-chain binding protein that facilitates interaction of ubiquitinated RIPK1 in Complex I with TAK1, leading to NFκB activation and cell survival signaling. In deficiency of TAB2, TAK1 is proposed to form an alternative complex with RIPK1 that leads to recruitment of RIPK3 and necroptosis (Mihaly et al. 2014).

Based on our findings, VCP might be involved in degradation of TAB2 or facilitation of TAB2 dispensable TAK1-RIPK1 complexes. VCP might be required for the alternative TAK1-RIPK1 binding in HT-29 cells, whereas the same pro-death complex is readily formed in RAW cells even in the absence of VCP. Therefore, future studies should aim to characterize the exact function of VCP in the VCP-RIPK1 complex and determine how TAK1 and TAB2 expression are affected by VCP inhibition.

Chapter 5: Bibliography

Adams, J., and M. Kauffman (2004). "Development of the proteasome inhibitor Velcade (Bortezomib)." Cancer Invest. **22**(2): 304-11.

Asai, T., et al. (2002). "VCP (p97) Regulates NFκB Signaling Pathway, Which is Important for Metastasis of Osteocarcoma Cell Line." Jpn J Cancer Res. **93**: 296-304.

Bader, M. and H. Steller (2009). "Regulation of cell death by the ubiquitin-proteasome system." Curr Opin Cell Biol **21**(6): 878-884.

Bhatti, I. A., et al. (2017). "Identification of a synergistic combination of Smac mimetic and Bortezomib to trigger cell death in B-cell non-Hodgkin lymphoma cells." Cancer Lett **405**: 63-72.

Braun, R. J. and H. Zischka (2008). "Mechanisms of Cdc48/VCP-mediated cell death: from yeast apoptosis to human disease." Biochim Biophys Acta **1783**(7): 1418-1435.

Chen, D., et al. (2011). "Bortezomib as the First Proteasome Inhibitor Anticancer Drug: Current Status and Future Perspectives." Current Cancer Drug Targets **11**(3): 239-53.

de Almagro, M. C., et al. (2017). "Coordinated ubiquitination and phosphorylation of RIP1 regulates necroptotic cell death." Cell Death Differ **24**(1): 26-37.

Degterev, A., et al. (2005). "Chemical inhibitor of nonapoptotic cell death with therapeutic potential for ischemic brain injury." Nature Chemical Biology **1:** 112-19.

DiDonato, J. A., et al. (1997). "A cytokine-responsive IκB kinase that activates the transcription factor NF-κB." Nature **388** :548-54.

Dziedzic, S. A., et al. (2018). "ABIN-1 regulates RIPK1 activation by linking Met1 ubiquitylation with Lys63 deubiquitylation in TNF-RSC." Nat Cell Biol **20**(1): 58-68.

Fulda, S., and D.Vucic (2012). "Targeting IAP proteins for therapeutic intervention in cancer." Nature Reviews Drug Discovery **11**: 109–124.

Geng, J., et al. (2017). "Regulation of RIPK1 activation by TAK1-mediated phosphorylation dictates apoptosis and necroptosis." Nat Commun **8**(1): 359.

Gorska, M. M., et al. (2007). "MK2 controls the level of negative feedback in the NF-kappaB pathway and is essential for vascular permeability and airway inflammation." J Exp Med **204**(7): 1637-1652.

Hayden, M. S. and S. Ghosh (2008). "Shared principles in NF-kappaB signaling." Cell **132**(3): 344-362.

He, S., et al. (2009). “Receptor interacting protein kinase-3 determines cellular necrotic response to TNF-alpha.” Cell **137** :1100-11.

Hideshima, T., et al. (2009). "Bortezomib induces canonical nuclear factor-kappaB activation in multiple myeloma cells." Blood **114**(5): 1046-1052.

Hildebrand, J. M., et al. (2014). "Activation of the pseudokinase MLKL unleashes the four-helix bundle domain to induce membrane localization and necroptotic cell death." Proc Natl Acad Sci U S A **111**(42): 15072-15077.

Jaco, I., et al. (2017). "MK2 Phosphorylates RIPK1 to Prevent TNF-Induced Cell Death." Mol Cell **66**(5): 698-710 e695.

Li, J., et al. (2012). "The RIP1/RIP3 necrosome forms a functional amyloid signaling complex required for programmed necrosis." Cell **150**(2): 339-350.

Magnaghi, P., et al. (2013). "Covalent and allosteric inhibitors of the ATPase VCP/p97 induce cancer cell death." Nat Chem Biol **9**(9): 548-556.

Mandal, P., et al. (2014). "RIP3 induces apoptosis independent of pronecrotic kinase activity." Mol Cell **56**(4): 481-495.

Mihaly, S. R., et al. (2014). "TAK1 control of cell death." Cell Death Differ **21**(11): 1667-1676.

Moquin, D. M., et al. (2013). "CYLD deubiquitinates RIP1 in the TNFalpha-induced necrosome to facilitate kinase activation and programmed necrosis." PLoS One **8**(10): e76841.

Morioka, S., et al. (2014). "TAK1 kinase switches cell fate from apoptosis to necrosis following TNF stimulation." J Cell Biol **204**(4): 607-623.

Moriwaki, K. and F. K. Chan (2016). "Regulation of RIPK3- and RHIM-dependent Necroptosis by the Proteasome." J Biol Chem **291**(11): 5948-5959.

Onizawa, M., et al. (2015). "The ubiquitin-modifying enzyme A20 restricts ubiquitination of the kinase RIPK3 and protects cells from necroptosis." Nat Immunol **16**(6): 618-627.

Sun, L., et al. (2012). “Mixed Lineage Kinase Domain-Like Protein Mediates Necrosis Signaling Downstream of RIP3 Kinase.” Cell **148 (**1-2): 213-27.

Sun, X., et al. (2002). "Identification of a novel homotypic interaction motif required for the phosphorylation of receptor-interacting protein (RIP) by RIP3." J Biol Chem **277**(11): 9505-9511.

Varfolomeev, E., et al. (2007). "IAP antagonists induce autoubiquitination of c-IAPs, NF-kappaB activation, and TNFalpha-dependent apoptosis." Cell **131**(4): 669-681.

Wang, L., et al. (2008). "TNF-alpha induces two distinct caspase-8 activation pathways." Cell **133**(4): 693-703.

Wang, Q., et al. (2006). "Regulation of retrotranslocation by p97-associated deubiquitinating enzyme ataxin-3." JCB **174**(7): 963.